

THE DETECTION AND MEASUREMENT OF IMPACT DAMAGE IN THICK CARBON FIBRE REINFORCED LAMINATES BY TRANSIENT THERMOGRAPHY (TT)

R J Ball* and DP Almond

Dept. of Materials Science and Engineering
University of Bath, Bath BA2 7AY

***Currently:- Department of Architecture and Civil Engineering, University of Bath,
01225386944, r.j.ball@bath.ac.uk**

ABSTRACT

The TT images from the impact face and rear face of impact damaged 3.44, 8.66 and 13.76mm thick composites are compared with the corresponding UCS images. Comparisons of delamination area and size were made using novel image analysis techniques. The defect sizes were also compared with crack lengths obtained from a selected number of specimens that were energy was proportional to the sectioned. Results showed that for all composite thicknesses the UCS damage area was proportional to the impact energy. The damage area obtained by TT from the front faces of the specimens did not correlate to the UCS damage areas although there was a correlation for the rear face damage on 3.44 and 6.88mm thick specimens. Crack lengths obtained from sectioning showed that UCS damage length was equal to the maximum crack length and back and front sub surface cracks corresponded to back and front TT images.

Key Words:- Thermography, Composite Materials, Impact, Damage.

INTRODUCTION

Composites are a widely used engineering material. The performance of a component through its life will be of particular importance to the engineer. This will be affected by the type of damage and loading sustained. Impact damage is one of the most significant types since this

can initiate delamination if the impact energy is above a critical value. Delamination within a composite can greatly reduce the compressive and fatigue strengths of the component.

Ultrasonic C-Scan (UCS) is a well established technique and has the ability to detect and quantify delamination damage in all thicknesses of composites. However it has the distinct disadvantages of being intrinsically slow and requiring a coupling agent.

Transient Thermography ^[1] is a less common NDT technique but has the advantage of being significantly faster means of obtaining a defect image. The main disadvantage of TT is that it can only detect damage near the surface (within ≈ 1 mm). The ability of TT to detect and quantify damage in thin CFRP laminates approx. 2mm has been successfully demonstrated. ^[2,3] This is because the depth of the damage is close to the surface and within the detection range of TT.

This paper describes work to quantitatively assess the ability of TT to detect impact damage in thick composites ranging from 3.44 -13.76mm. Initially there were doubts as to whether the technique would work as the depth, severity (thickness) and distribution of the delaminations in the material were not known. The approach undertaken was to produce TT images for a range of samples of varying thickness and delamination area and then to compare these with UCS images which were used as a reference. TT images were produced for the front (impacted face) and the back of the specimens. A small number of the samples were sectioned in order to obtain information on the damage distribution through the thickness of the sample. The lengths of the cracks revealed by this were then compared with the corresponding length across the defect on TT and UCS images. Because a prime application for these materials is the aircraft industry, half of the specimens were painted with a standard aircraft finish paint in order to assess the effect of paint on the effectiveness of TT.

Thin composites have been used for many years in manufacture aircraft components. In order to produce more integrated designs attempts have been made to use thick composites for large primary load bearing structures within the airframe such as a wing box. This has increased the need for reliable NDT techniques which can quickly assess the integrity of these components since damage tolerance is important. Much of earlier imaging has been performed on

comparatively thin ($\approx 2\text{mm}$ thick) composites whilst this work has concentrated on much thicker composites.

SAMPLES

Two composite laminates of dimensions $350 \times 350\text{mm}$ of each laminate thickness were produced. The laminates were then C-scanned for quality. One of each thickness plate produced was then painted using an epoxy based primer and a flexible polyurethane top coat. Six $150 \times 100\text{mm}$ specimens were cut from each panel. The laminates were manufactured using a Fiberdux 914C epoxy resin and triaxial blankets of non crimp fabric (NCF) reinforcement. Each triaxial blanket was found to be equivalent to 0.86mm of the total thickness of the finished laminate. Two variants of each blanket were produced, (variant A: $-45/+45/0$ and B: $+45/-45/0$). This allowed symmetrical and balanced laminates to be constructed by combining these two types. Figure 1. shows how a single unit is constructed. These units were then stacked to produce laminates containing 4, 8 and 16 blankets, giving average laminate thicknesses of 3.44 , 6.88 and 13.76mm respectively.

TECHNIQUES

Impacting of Specimens

Specimens were impacted using a Rosand Instrumented Falling Weight Impact Tester, Type 5. All impacts were carried out at low impact velocity, i.e. less than 3ms^{-1} . In order to keep the impact velocities below this limit the mass above the striker was varied as appropriate. When using the testing machine a target energy is selected and the actual impact energy achieved was displayed after the impact. A 20mm hemispherical diameter striker was used for all the impacts. After the initial impact the striker head was caught to prevent any subsequent impact. All results are for single impact events. Specimens were simply supported around their edge during impacting and retained using four clamps, two positioned each side along the specimens length. Three different impact energies were selected for each laminate thickness, low, medium and high. The lowest energy corresponded to the threshold energy below which no delamination will be initiated. The maximum energy that could be adsorbed by the plate before destruction (penetration of striker into composite or delaminations reaching outer edge of specimen) is referred to as the high energy and the medium energy is the midway point between

the two. Typical impact energies for the three thicknesses of composites are indicated in table 1.

Transient Thermography

The IR Camera used was a Thermovision 750 camera, manufactured by BG Agema Infrared System AB, Sweden. This utilises a liquid nitrogen cooled indium antimonide (InSb) photovoltaic detector which produces a resolution of 0.2°C at 30°C object temperature, and a spectral response of 2 - 5.6µm.

Each camera frame is produced from 4 interlaced fields, each containing 100 scanning lines. 70 of these lines are used to produce each frame, therefore each frame is constructed from 280 lines in total. The camera is able to scan at a rate of 25 fields per second, allowing it to image approximately 6 frames per second.

Specimens were heated using two 500W flood lamps mounted horizontally each side of the specimen. The 'after glow' from the lamps was screened by mechanical shutters synchronised to the flash system. Crossed optical benches were used to hold the specimen, camera and lamps in position during the imaging process.

A digitised modular frame grabber mounted in a 486-PC was used to record the images. The PC was able to record up to 24 frames (images), each consisting of 256x248 pixels. The heating time was controlled using an Amstrad 80862 PC.

The damage areas were then obtained from the images using the image analysis technique described below.

Typical back and front face TT images for 4,8 and 16 blanket specimens are shown in figures 2-4. The 4 and 8 blanket specimens shown are for high energy impacts whereas the 16 blanket is for a low energy impact. The images clearly show the different sizes and shapes of damage produced.

Ultrasonic C-Scan

The ultrasonic C-scans were produced using the pulse echo technique at a frequency of 5MHz. Signal threshold levels were chosen so that the damage area appeared as white against the remainder of the trace. A typical image is shown in Figure 5. The defect can be identified as the white area in the centre of the image surrounded by grey bands. The darker surrounding area is the undamaged material. A Taymaya digital planimeter was used to determine the damage areas from 'to scale' printed images by following the outer band.

Sectioning

One of each laminate thickness was sectioned along to 0° fibre direction which corresponded to the length of the specimen. Photo micrographs were then produced by photographing the polished samples and scanning the photos into a computer to allow the delamination and interply cracks to be highlighted.

EXPLANATION AND ILLUSTRATION OF IMAGE ANALYSIS

The sizes of the delaminations shown by the images obtained from TT were determined using an image analysis technique. The image processing package used was Optimas 6. ^[4]

Two different views of samples were used depending on the impact energy. The close up views for low impact energies were calibrated by attaching a piece of thin metal sheet of exactly 25mm in width to the sample so that it could be seen in the top of the image. Large images were used for medium and high energies and calibrated using the edges of the sample as reference points.

Edges of subsurface delaminations producing the thermal images were taken to be the locus of points corresponding to the full width at half maximum (FWHM) of the defect image contrast. This approach follows theoretical work and experimental studies of model defect samples. ^[5,6]

In order to calculate a FWHM value of a real defect image, so a damage area could be obtained, an image analysis macro was written. This worked as follows; A line of boxes of specified dimensions and number, was drawn across the brightest point on the damage area. Box sizes 0.5mm for whole width images and 0.25mm for close up images were used. The mean grey scale value from each box was then calculated. The smallest and largest means were used to calculate the threshold value by the FWHM method. Figure 6a shows the initial image. Figure

6b shows the image with the line of boxes drawn across the brightest point. The mean value from each box is shown in Figure 7. Figure 6c shows the FWHM line around the defect image.

There were two main factors which reduced the accuracy of this method for calculating the defect area. The first being the varying intensity within the defect image relative to the background and the effect of 'overheating' which occurred at the edges of the specimens,. An example of this is shown in Figure 8b. The second was the fact that the IR camera scanned in 4 fields, horizontal scanning lines were produced on the image. This caused a 'bleeding' effect at the edges of the image this can be seen in figure 8b&c.

On a number of the specimens the brightness at the sample edges caused by overheating was comparable to that of the inner defect image. This resulted in the computer outlining the edge of the sample as well as the defect. Figure 8a&b show the TT image of an 8 blanket medium impact specimen with and without defect size as calculated by the computer superimposed on top. Figure 8c shows the recalculated defect area when using a region of interest (ROI) box.

The ease with which the defect size could be accurately calculated varied for different specimens.

QUANTITATIVE DEFECT IMAGE RESULTS

Figures 9a,b & c show the UCS damage area vs. impact energy for 4,8 and 16 blanket specimens. Figures 10 & 11 a,b & c are plots of front and back TT vs. UCS damage area damage area for 4,8 & 16 blanket specimens respectively.

EXPLANATION AND ILLUSTRATION OF DEFECT MEASUREMENT

Figures 12,13 and 14 show photo micrographs of the impact damage through 4, 8 & 16 blanket specimens. During microscopical examination of the sections the presence of interply cracks, which extended beyond that indicated on the photographic images and out to the edge of the defect denoted by the C-scan, were seen between the lower plys. These were not visible on the photographs or at low magnification ($\approx 10\times$) but could be seen at higher magnifications ($\approx 40\times$). Only the visible cracks have been identified on the photo micrographs. This shows that delamination damage cracks can occur which are barely visible under anything other than high

magnification microscopy. The general scheme of damage as seen in all laminate thicknesses is shown schematically in figure 15. Figure 16 shows a histogram which compares the length across the UCS and front and back TT images with sub-surface and maximum crack lengths measured from a 4,8 and two 16 blanket specimens.

7. CONCLUSIONS

The following conclusions can be drawn from the results presented. Measurements taken from sectioned specimens and UCS images showed that all delamination damage was detected by UCS. Plots of UCS damage area against impact energy showed a proportional relationship. TT images demonstrate the ability of the technique to detect the presence of damage in 4,8 and 16 Blanket CFRP specimens. The presence of paint on the surface of a sample does not have a significant effect on the ability of either of the methods to detect damage. The damage area estimated from the front face TT images did not correlate with that obtained from the UCS but did correlate with measurements of sub-surface damage obtained from sectioned samples. The damage areas produced by the back face TT images correlated well with that obtained from sectioned specimens and with UCS images for 4 and 8 blanket, but not 16 blanket specimens. From plots of TT damage area vs. UCS damage area there is evidence that a minimum threshold damage size exists which is not detectable by TT using the equipment and method applied in this work. Results have shown that TT is a potentially viable method for detecting impact damage in thick CFRP laminates. Thermographic techniques such as lock-in thermography that are capable of detecting defects at a greater depth are worth further investigation.

ACKNOWLEDGEMENTS

The authors would like to thank James Ball, BAe Airbus, Filton for supplying samples and general advice during the course of this work and Mark Deven, School of Materials Science and Engineering, University of Bath, Bath, for advice and guidance on using Optimas 6, image analyser.

REFERENCES

- [1] JM Milne and WN Renolds, 1984 SPIE *Proc.* **520** 119-22
- [2] Almond, D. P., Delpech, P., Beheshtey, M. H. and Peng, W., Quantitative determination of impact damage and other defects in carbon fibre composites by transient thermography. *SPIE*, 1996, **2944**, 256-264.
- [3] Krapez, J.-C. and Balageas, D. Early detection of thermal contrast in pulsed stimulated infrared thermography. *QIRT 94 Eurotherm Series 42* EETI ed., Paris, pp. 260-266.
- [4] *OPTIMAS 6.1*, Optimas UK Ltd., West Maling, Kent, UK.
- [5] DP Almond, SK Lau, Defect sizing by transient thermography. I. an analytical treatment, *J. Phys. D: Appl. Phys.* **27**, 1994
- [6] AR Hamzah, P Delpech, MB Saintey and DP Almond, *INSIGHT*, Vol. **38**, p168-170, 1996

| | Low Energy (J) | Medium Energy (J) | High Energy (J) |
|-------------------|-----------------------|--------------------------|------------------------|
| 4 Blanket | 4.5 | 7.2 | 12.5 |
| 8 Blanket | 9.5 | 16 | 27 |
| 16 Blanket | 38 | 56 | 75 |

Table 1 Typical impact energies for the three thicknesses of composite

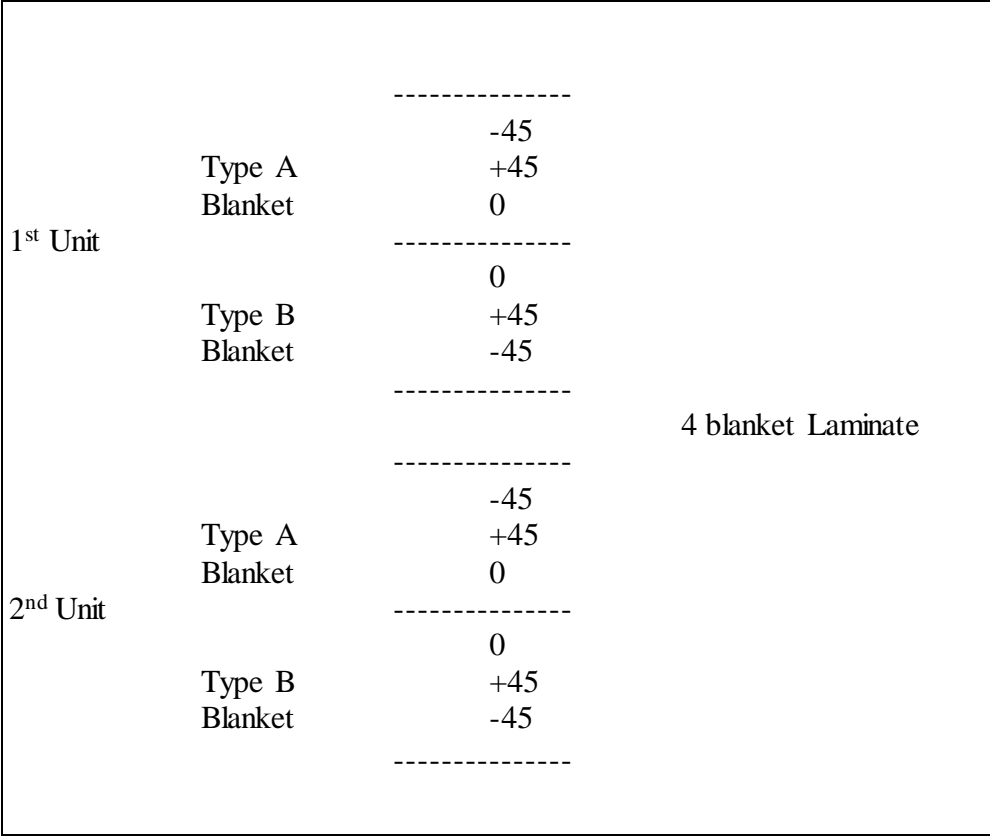


Figure 1 Lay-up of 4 blanket laminate

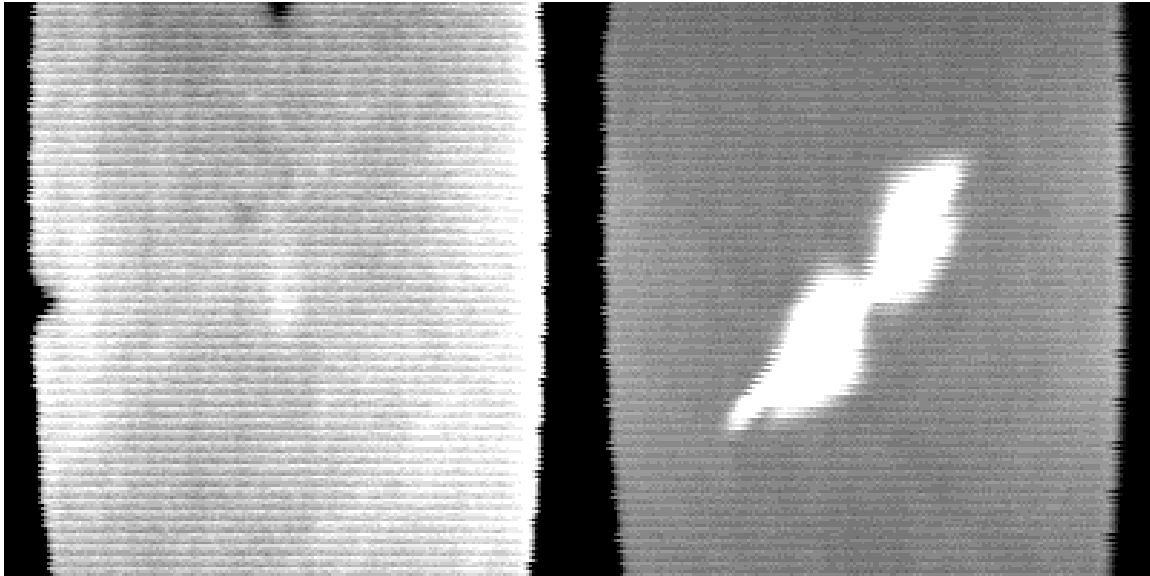


Figure 2 Front, a, and back, b, TT images of a 4 blanket, Painted, High energy impacted laminate

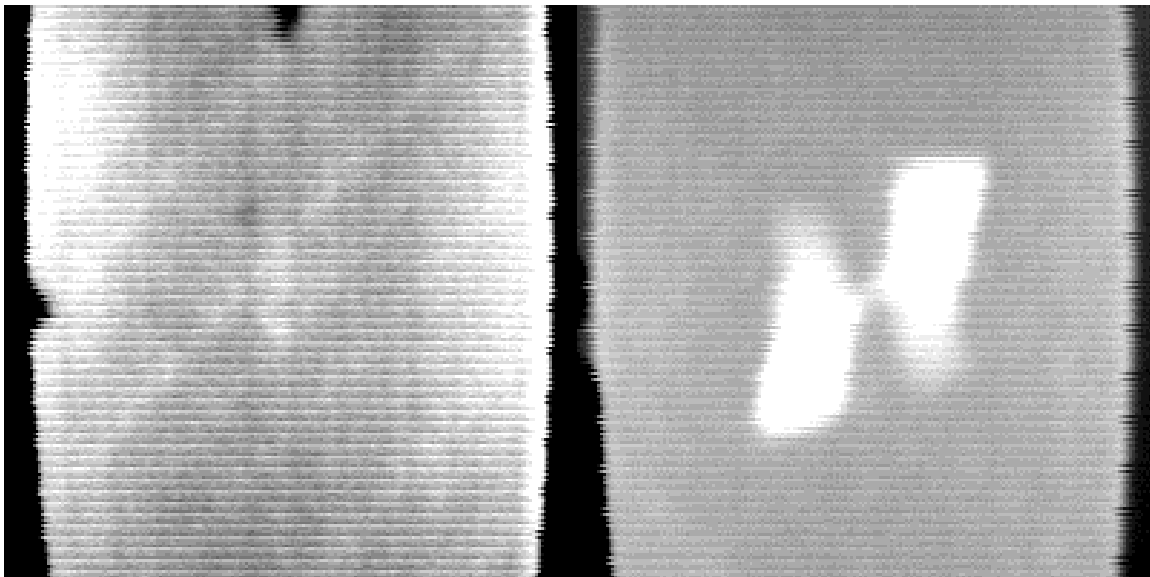


Figure 3 Front, a, and back, b, TT images of an 8 blanket, Painted, High energy impacted laminate

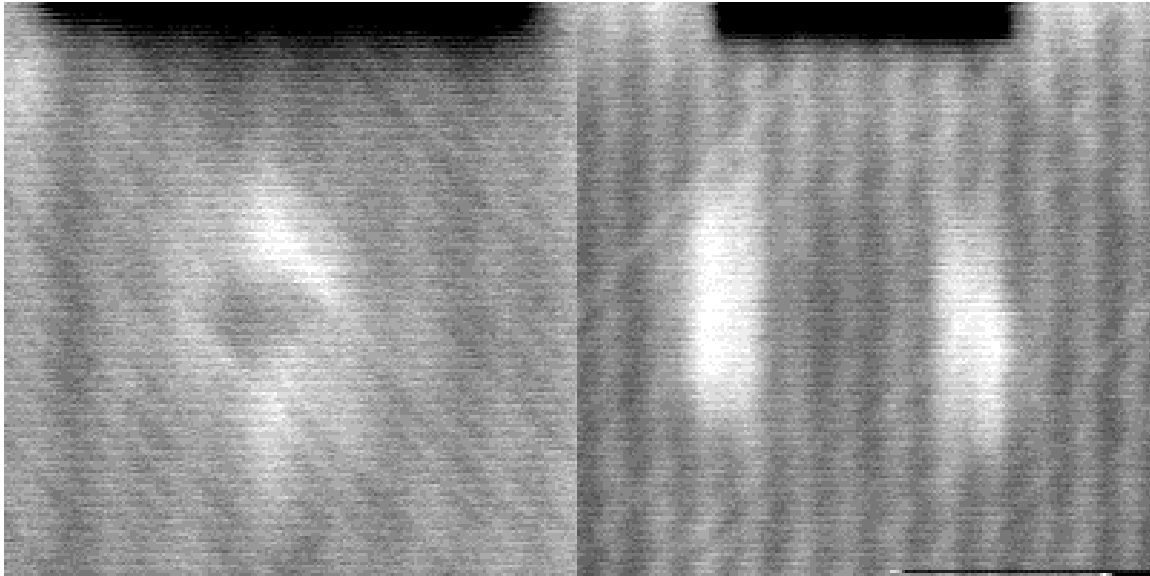


Figure 4 Front, a, and back, b, TT images of a 16 blanket, Low energy impacted laminate

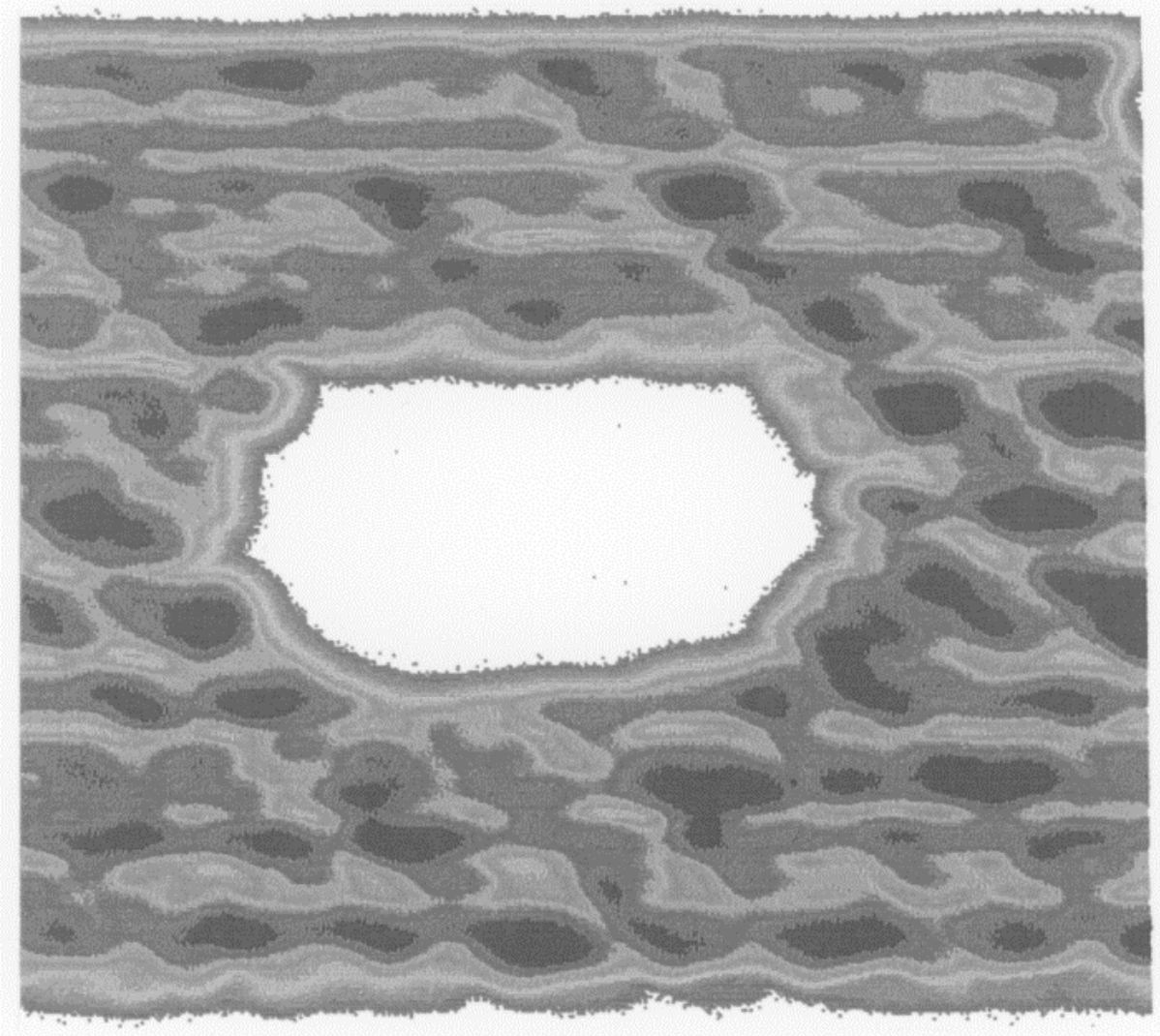


Figure 5 Typical UCS Image, 16 Blanket, Low energy

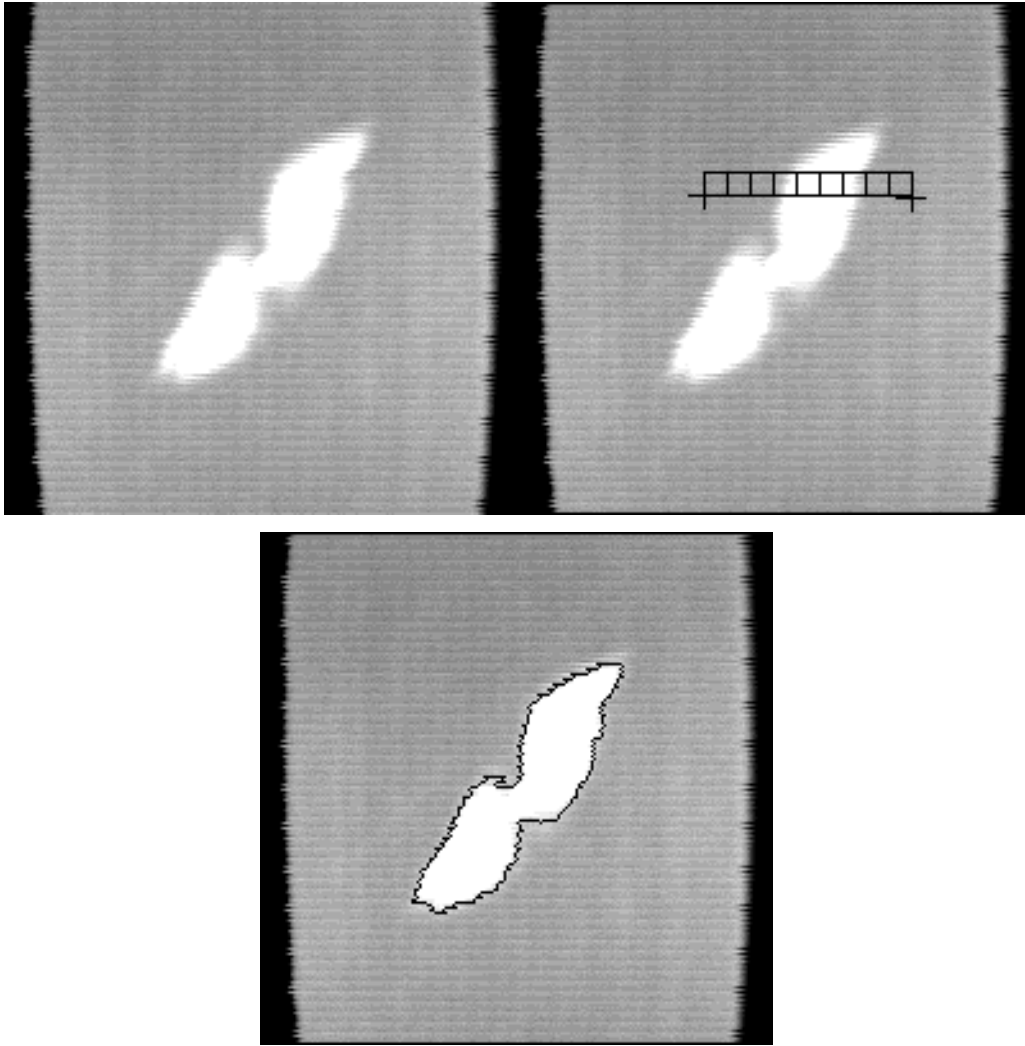


Figure 6 Sequence of images showing the identification of a defect using the Optamas 6 image analysis macro, see text

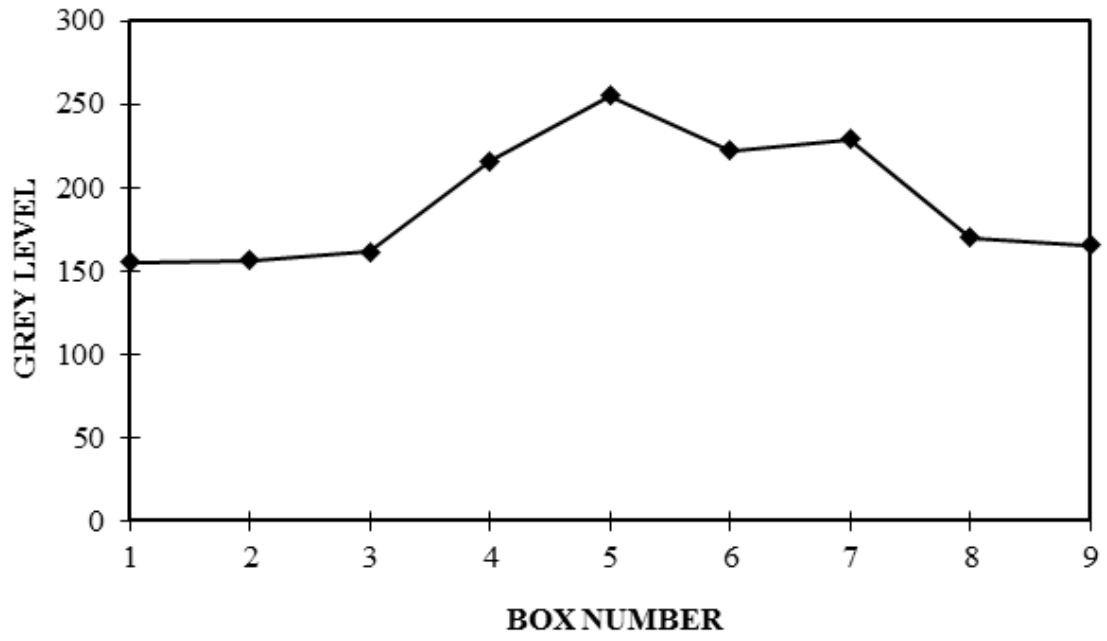


Figure 7 Plot showing mean grey level value in each box drawn across defect in figure

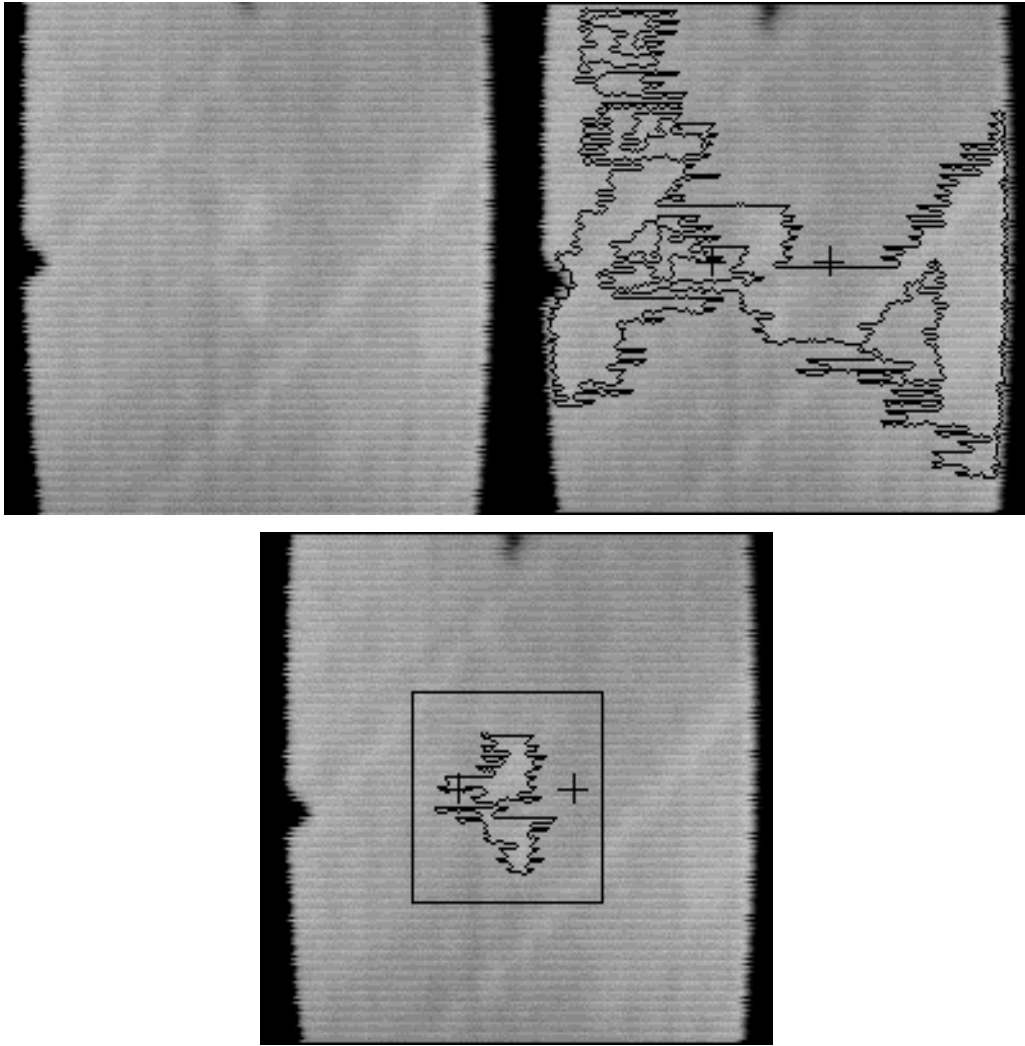


Figure 8 TT images showing defect, a, calculated defect area, b, and calculated defect area using ROI box, c

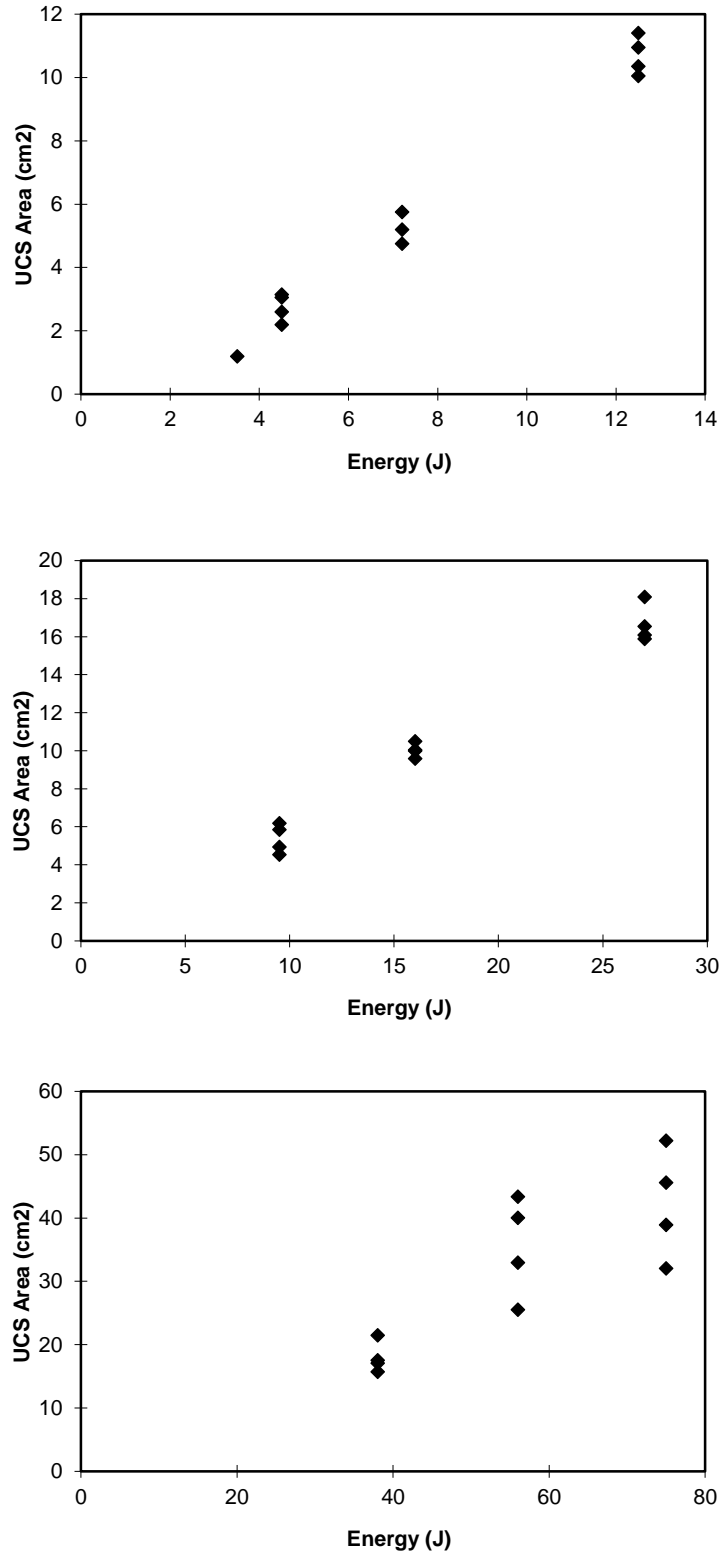


Figure 9 Plot of UCS area vs. impact energy for 4 blanket specimens, a, 8 blanket specimens, b, & 16 blanket specimens, c

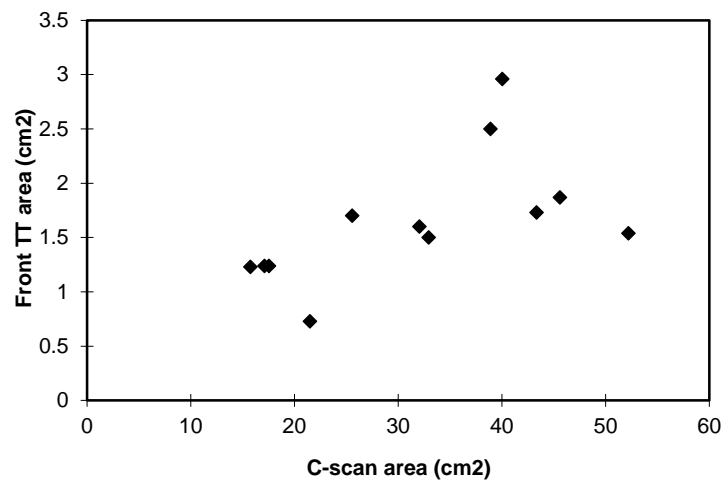
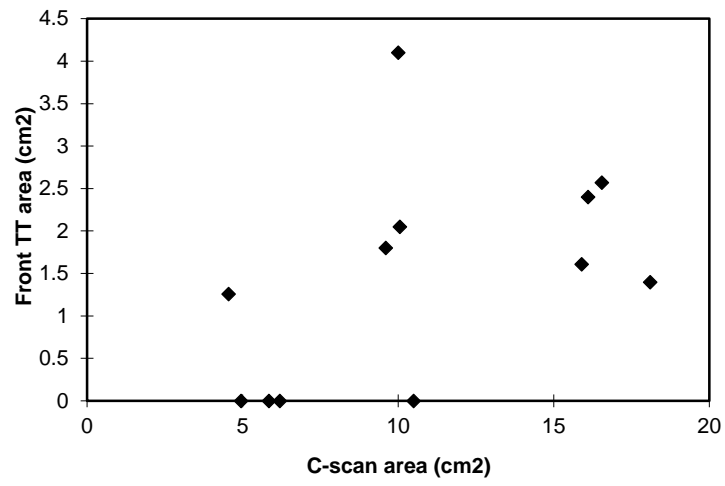
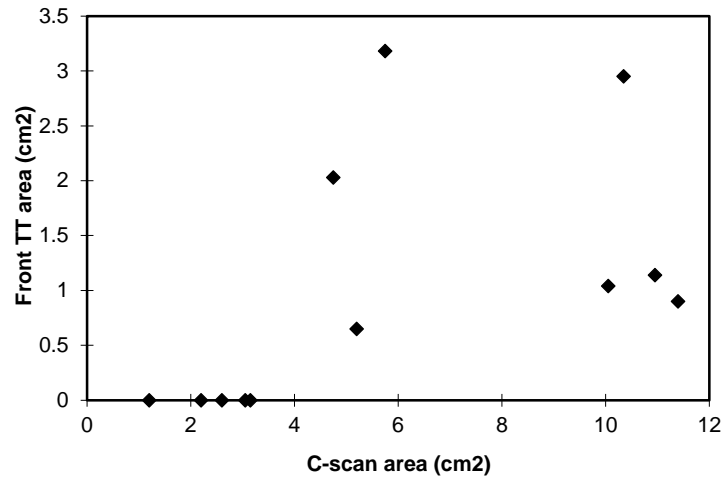


Figure 10 Plot of front TT area vs. UCS area of 4 blanket specimens, a, 8 blanket specimens, b, & 16 blanket specimens, c

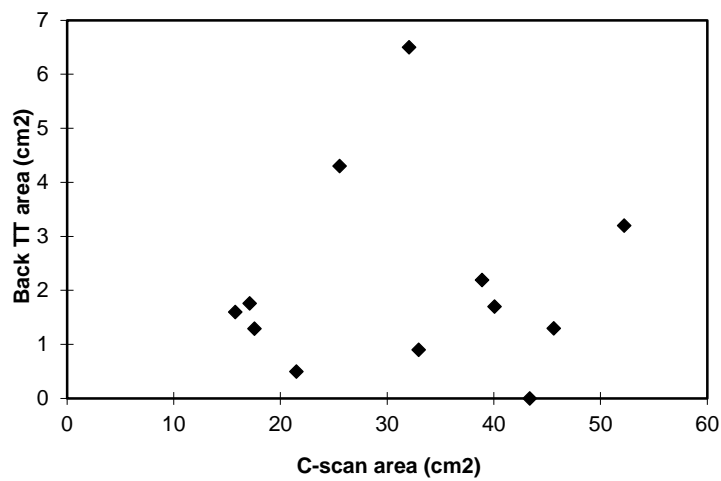
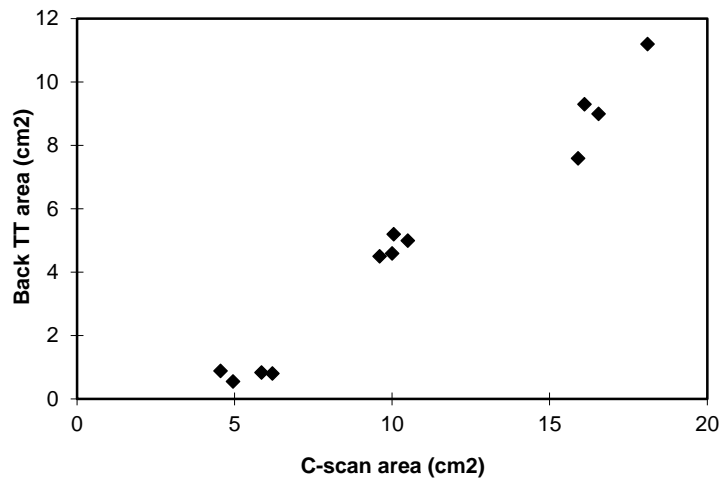
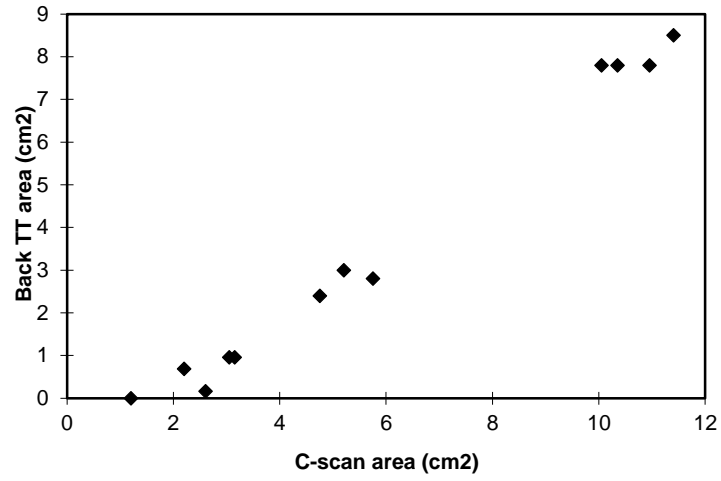


Figure 11 Plot of back TT area vs. UCS area of 4 blanket specimens, a, 8 blanket specimens, b, & 16 blanket specimens, c

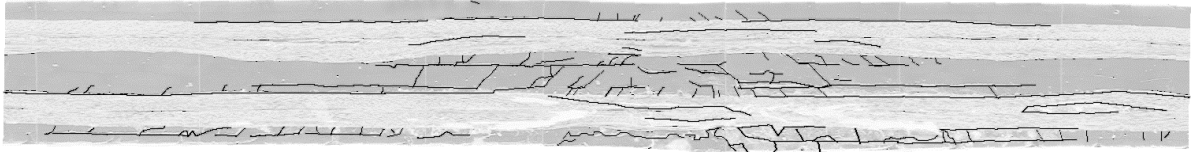


Figure 12 Photo micrograph showing crack network in a 4 blanket laminate

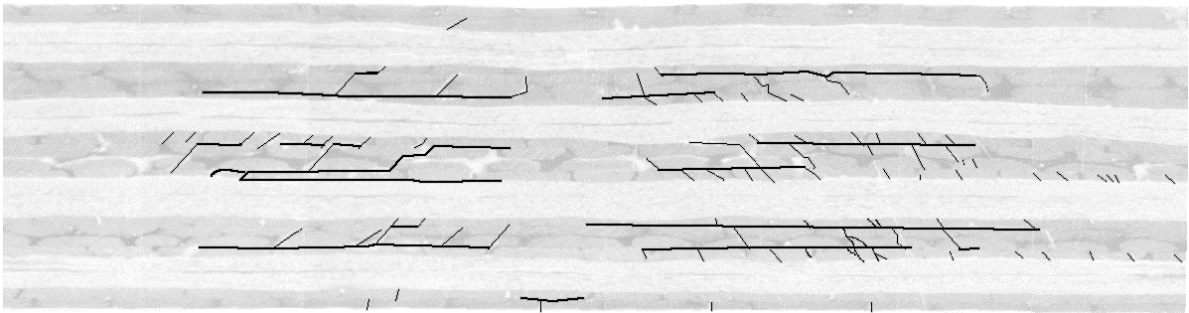


Figure 13 Photo micrograph showing crack network in a 8 blanket laminate

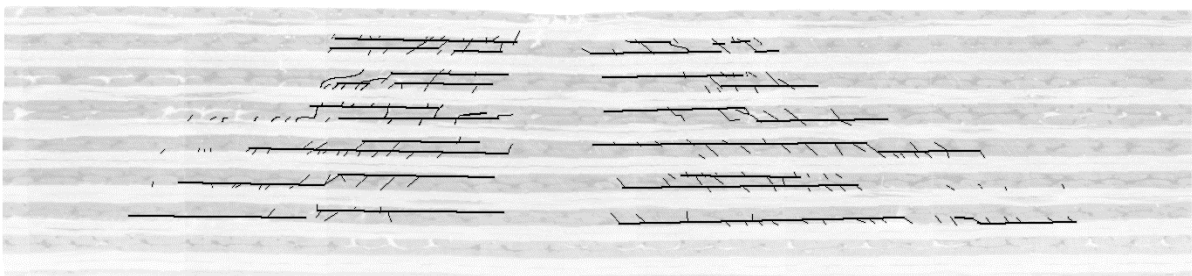
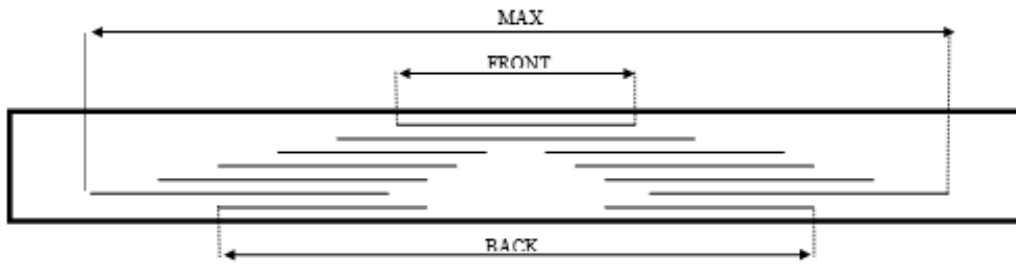


Figure 14 Photo micrograph showing crack network in a 16 blanket laminate



Specimen (max) = Maximum length of delamination identified from sectioned specimen.

Specimen (front) = Length of delamination identified from sectioning occurring closest to the specimen front.

Specimen (back) = Length of delamination identified from sectioning occurring closest to the specimens back.

Figure 15 Schematic of typical impact damage showing standard dimensions

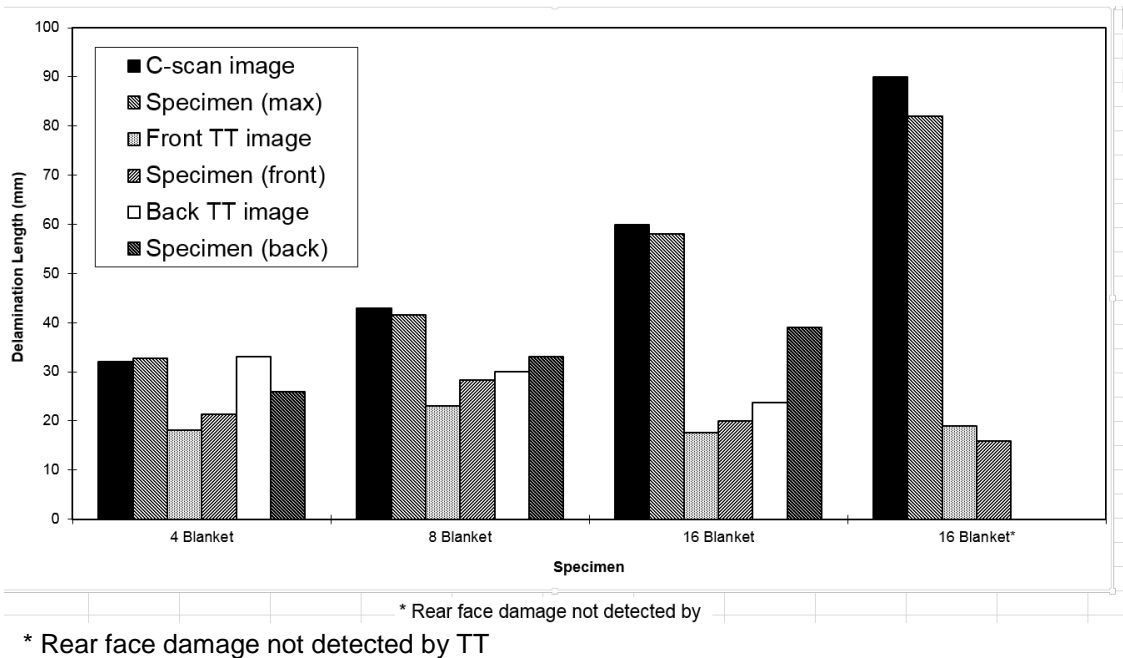


Figure 16 Histogram comparing length of damage as measured from sectioned specimen with damage length obtained from TT and UCS images